



Surface topography index: a novel deformity severity assessment index for pectus excavatum

Hui Wang^{1,2#}, Wei Liu^{2#}, Dong-Ying Zhang^{3#}, Wen-Yue Si², Qing-Lin Yang², Lian-Wei Lu², Feng-Hua Wang², Le Li², Qi Wang⁴, Hui-Min Xia^{1,2}

¹The Second School of Clinical Medicine, Southern Medical University, Guangzhou, China; ²Department of Pediatric Surgery, Guangzhou Women and Children's Medical Center, Guangzhou Medical University, Guangzhou, China; ³National Clinical Research Center for Respiratory Disease, The First Affiliated of Guangzhou Medical University, Guangzhou, China; ⁴Department of Forensic Pathology, Southern Medical University, Guangzhou, China

Contributions: (I) Study concepts and design: H Wang, Q Wang, HM Xia; (II) Guarantors of the integrity of the entire study: W Liu, HM Xia; (III) Clinical studies: H Wang, QL Yang, LW Lu, FH Wang, L Li, W Liu; (IV) Literature research: H Wang, DY Zhang, WY Si; (V) Statistical and data analyses: H Wang, DY Zhang, WY Si; (VI) Manuscript preparation: All authors; (VII) Manuscript editing: All authors.

#These authors contributed equally to this work.

Correspondence to: Hui-Min Xia. The Second School of Clinical Medicine, Southern Medical University, Guangzhou, China. Email: xia-huimin@foxmail.com; Qi Wang. Department of Forensic Pathology, Southern Medical University, Guangzhou, China. Email: wangqi1980@smu.edu.cn.

Background: The surface topography index (STI) has great potential in both routine computed tomography (CT) scan and emerging optical imaging systems. However, the diagnostic accuracy and stability of the STI as a deformity severity assessment index has not been fully confirmed. Therefore, the aim of the present study was to determine the diagnostic performance of the STI as a novel deformity severity assessment index for pectus excavatum.

Methods: The present study consisted of 722 chest CT images from a single center. The standard CT index (CTI) and STI were calculated for all patients. The between-group difference and the level of compliance between the CTI and STI was analyzed by *t*-test and Pearson correlation. The diagnostic value and optimum discriminatory values of the CTI and STI were calculated by a receiver-operating characteristic (ROC) curve and DeLong's test.

Results: The distributions of the CTI and STI were similar and showed a slight overlap between the pectus excavatum (PE) and non-PE groups. Both the CTI and STI significantly differed between the 2 groups ($P < 0.001$). The STI demonstrated a strong Pearson correlation with the CTI ($r = 0.91$, 95% confidence interval: 0.88–0.91, $P < 0.001$). The ROC curves showed that STI = 1.58 (sensitivity: 0.93, specificity: 0.95) could be considered equivalent to CTI = 2.72 (sensitivity: 0.93, specificity: 0.97) as the optimum discriminatory values. DeLong's test showed no significant difference in the ROC curve results between the CTI and STI ($Z = 0.90$, $P = 0.37$).

Conclusions: The STI has comparative discrimination ability in PE diagnosis and deformity severity assessment when used with the standard CTI. The STI as a novel index is not only an ideal evaluation metric of PE deformity but also an objective trait for PE patients just as weight and height for everyone.

Keywords: Pectus excavatum; surface topography index (STI); computed tomography index (CTI); diagnosis; assessment.

Submitted Jun 04, 2021. Accepted for publication Aug 02, 2021.

doi: 10.21037/tp-21-282

View this article at: <https://dx.doi.org/10.21037/tp-21-282>

Introduction

Pectus excavatum (PE) is the most common congenital chest wall deformity and is characterized by a visible depression in the sternum (1). PE deformities may constrict cardiopulmonary development in children and lead to heart displacement and obstructive pulmonary disease (2). Medical intervention is necessary in severe PE cases. Computed tomography (CT) scan has been the most widely used method to assess the severity of PE deformation. A CT index (CTI) greater than 3.25 has been the gold standard indication for intervene since 1987 (3). However, high-dose ionizing radiation severely restricts the frequency of CT scans (4). Unfortunately, PE deformities may worsen as the children grow, thereby repeated and regular evaluations are required. The gap between evaluation needs and technical limitations has resulted in a series of unresolved issues in PE, such as its critical cause factors.

Surface topography (ST) scans based on optical imaging systems have been applied to assess the severity of PE deformities (5-8). In 2007, Poncet *et al.* first used the InSpeck system, which comprises 4 digitizers, to assess 5 patients with PE (5). In 2009, Glinkowski *et al.* investigated 3D optical images of 12 PE cases utilizing systems based on 4 digital light-processing projectors (6). In 2019, Taylor and colleagues measured the topographic mapping of chest wall deformities in 42 PE patients using a portable, hand-held scanner with 1 camera (7). The advantage of optical imaging systems is to capture the 3D surface information without radiation. Fortunately, the characterized configuration of PE deformities is visible on the surface. In previous studies, the correlation coefficients (r) were all strong and are as follows: 0.97 ($r^2=0.94$), 0.93 ($r^2=0.87$), and 0.85 ($r^2=0.72$), respectively (5-7). The above results were similar: there was a strong linear correlation between the novel index based on optical imaging systems and the standard CTI. However, the correlation coefficients decreased sharply (from 0.97 and 0.93 to 0.85) as the number of PE cases increased (from 5 and 12 to 42). It is entirely possible that the correlation coefficient continue to weaken as the number of patients further increases. Moreover, the ST scanners involved diverse optical imaging systems with different parameters. The apparatuses used by Poncet *et al.* and Glinkowski *et al.* were stationary, large, expensive, and not suitable for general application (5,6). Taylor *et al.* used a portable Artec Eva 3D scanner in their study. The downside of this method was that the correlation coefficient decreased from over 0.87 to 0.72 (7). Although the correlation was still strong, the feasibility and generalization of this ST model became

unclear. Both subject number and equipment used are uncertainty factors of ST scans.

The establishment of a scientific evaluation index system will contribute to assessing the severity of PE deformities accurately and comprehensively. Given the abovementioned uncertainties, to determine the accuracy and stability of the ST index (STI) system is very important. As an emerging technique, ST scans vary in size, cost, and accuracy parameters. In contrast, CT scanners have stable components and user-friendly control, and CT scans have been used in regular examinations worldwide. The digital data derived from CT scans are the most reliable for testing a novel index system in PE evaluation. Although ST scans based on visible light only capture surface information, CT scans based on X-ray can obtain not only the internal structure but also surface data. Therefore, both the CTI and STI could be measured on CT images. Moreover, when the STI is derived from CT images, the only variable is the calculation. Changing 1 variable at a time also conforms to the designed principle of the scientific method. We hypothesized that the STI has the ability to diagnose PE and assess depression severity in the sternum. We performed the present comparative study to test the discrimination ability of the STI and its diagnostic consistency with the standard CTI in PE evaluation.

We present the following article in accordance with the STARD reporting checklist (available at <https://dx.doi.org/10.21037/tp-21-282>).

Methods

Patients and criteria

The study population randomly included 722 children who underwent chest CT scans between January 2013 and September 2017. All patients or their parents provided signed informed consent. Patient characteristics were acquired (3).

The exclusion criterion for the PE group were patients with other combined diseases and deformities. The median age for the 371 PE patients in total was 5 years (3.6–9 years); 275 patients were male. The exclusion criteria for the control group were as follows: (I) patients with chest wall abnormality; (II) patients with scoliosis; and (III) patients with chest wall trauma. The median age of the 351 patients was 3 years (1–7 years) in the non-PE group; 226 patients were male. The clinical indication for CT scans in the non-PE group is listed in *Table 1*.

Definitions and data acquisition

CT scans were performed using Aquilion 64 (Aquilion Vision; Toshiba, Tokyo, Japan), and CT imaging data were independently reviewed by a pediatric surgeon and a pediatric radiologist. The CTI and STI were calculated for all patients. The CTI was defined as the maximum transverse inner diameter of the chest divided by the minimum distance between the posterior sternum and the anterior spine through the deepest-level CT image of the PE deformity. The STI was defined as the maximum

transverse outer diameter of the chest divided by the maximum anterior–posterior distance from the front of the sternum to the back of the vertebral body with the most depressed topography (Figure 1). For the non-PE children, the CTI and STI were acquired at the level of the upper margin of the xiphoid process.

Statistical analysis

Continuous variables (i.e., the CTI and STI) are described as the mean \pm standard deviation or median and quartile, and were analyzed using an independent samples *t*-test. A Pearson correlation coefficient analysis was performed to analyze the compliance between the CTI and STI. Receiver-operating characteristic (ROC) curves were generated to graphically display the discriminatory accuracy and to determine the optimum discriminatory values of the CTI and STI. DeLong' test was used to analyze the differences between the 2 ROC curves. The statistical analysis was performed with R software version 3.3.1 (University of Auckland in New Zealand, Auckland, North Island, New Zealand). $P < 0.05$ was considered statistically significant.

Ethical approval

All procedures performed in this study involving human participants were in accordance with the Declaration of

Table 1 Clinical indications for the control group

No.	Clinical indications for CT scans	Number of cases
1	Bronchopulmonary cyst	72
2	Pulmonary abscess	65
3	Mediastinal mass	59
4	Bronchopneumonia	39
5	Trauma	35
6	Pulmonary tumors	28
7	Empyema	23
8	Diaphragmatic eventration	19
9	Esophageal cyst	6
10	Chylothorax	5

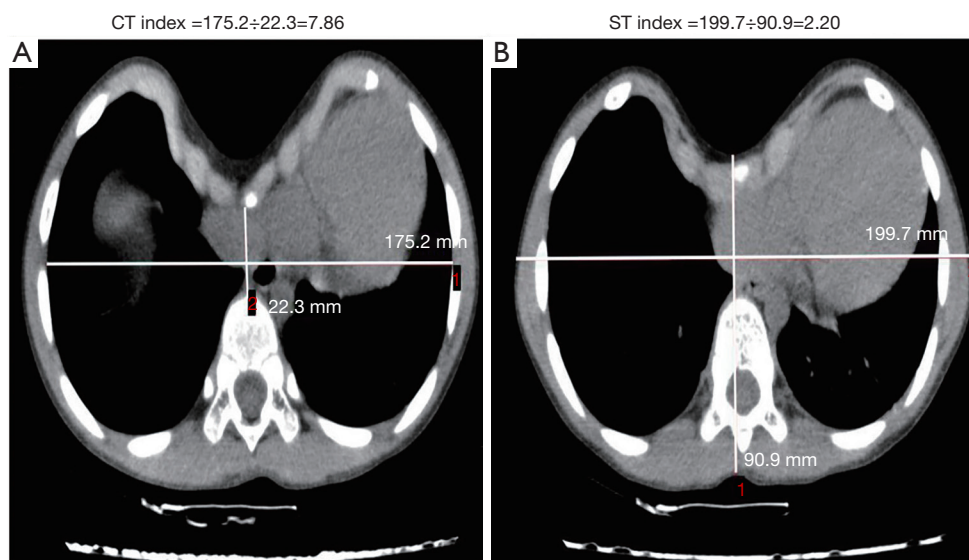


Figure 1 Definition of the computed tomography (CT) index and surface topography (ST) index. Calculations of the CT index (A) and ST index (B).

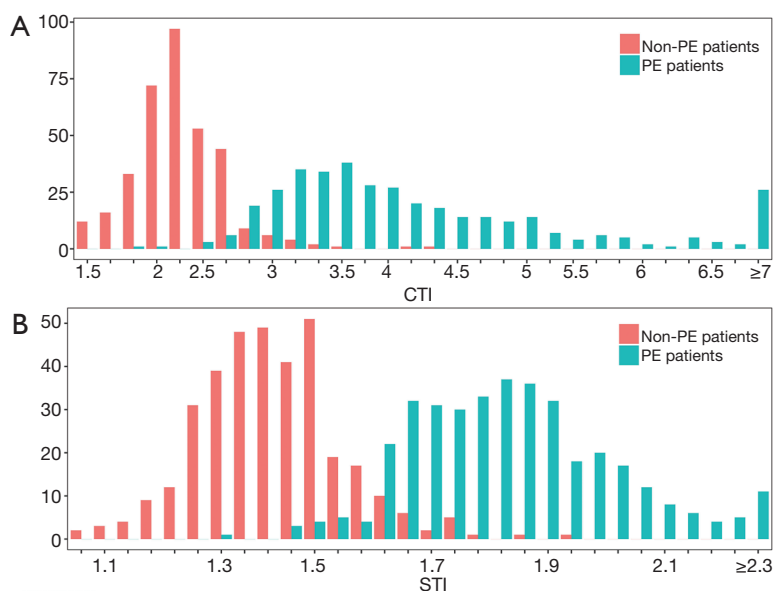


Figure 2 Distribution of the computed tomography index (CTI) (A) and surface topography index (STI) (B). Distributions were similar and showed a slight overlap between pectus excavatum (PE) patients and non-PE patients. Both the CTI and STI showed significant differences between the PE group and non-PE group ($P < 0.001$)

Table 2 Comparison of the CTI and STI between PE and Non-PE groups

	PE group (n=371)	Non-PE group (n=351)	P value ^a
CTI	4.13±1.18	2.26±0.37	<0.001 [*]
STI	1.83±0.18	1.40±0.13	<0.001 [*]

Presented as mean ± standard deviation (range). ^{*}, statistically significant ($P < 0.05$). ^a, independent samples *t*-test. CTI, computed tomography index; PE, pectus excavatum; STI, surface topography index.

Helsinki (as revised in 2013). This retrospective study was approved by the institutional review board of Guangzhou Women and Children’s Medical Center on November 18, 2016 (No. 2016111876). Written informed consent was obtained from the patients or their parent. Clinical Trial Registration: A cohort study of pectus excavatum in children (ChiCTR-ROC-17013308).

Results

Comparison of the CTI and STI between PE and non-PE groups

The mean CTI was 4.13±1.18 and the mean STI was 1.83±0.18 for the 371 PE patients, while the mean CTI was

2.26±0.37 and the mean STI was 1.40±0.13 for the 351 non-PE children. The distributions of the CTI and STI between the PE and non-PE groups were similar and showed a slight overlap between the 2 groups (Figure 2). Both the CTI and STI showed significant differences between the PE group and non-PE group ($P < 0.001$) (Table 2).

Diagnostic consistency between the CTI and STI

The STI demonstrated good compliance with the CTI. The STI demonstrated a strong Pearson correlation with the CTI for all 722 participants ($r = 0.91$, 95% confidence interval: 0.88–0.91, $P < 0.001$). The fitted, monotonically increasing curve showed that the STI increased as the CTI increased as follows: $CTI = -2.15 \times STI + 1.85 \times STI^2 + 1.68$ (Figure 3). Based on the fitted formula, $STI = 1.67$ could be considered equivalent to $CTI = 3.25$.

Diagnostic performance of the CTI and STI

The area under the ROC curve of the CTI and STI was 0.982 (0.973–0.991) and 0.978 (0.969–0.987), respectively (Figure 4). Regarding the CTI, when the optimal ROC value was 2.72, the specificity and sensitivity were 0.93 and 0.97, respectively. Regarding the STI, the optimal ROC value was 1.58, and the specificity and sensitivity were 0.93

and 0.95, respectively. The ROC curves showed that STI =1.58 (sensitivity: 0.93, specificity: 0.95) could be considered equivalent to CTI=2.72 (sensitivity: 0.93, specificity: 0.97) as the threshold value for distinguishing PE patients from non-PE individuals (Figure 4). DeLong's test showed no significant difference between the ROC results of the CTI and STI ($Z=0.90$, $P=0.37$).

Discussion

Our study used a large database of 722 patients over a period

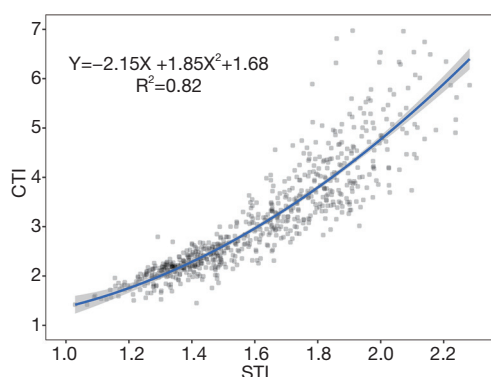


Figure 3 Correlation between the computed tomography index (CTI) and surface topography index (STI). STI demonstrated a strong Pearson correlation with the CTI in all 722 participants ($r=0.90$, 95% confidence interval: 0.88–0.91, $P<0.001$). Fitted, monotonically increasing curve showed that the STI increased as the CTI increased.

of 4 years. We found that the STI has a discrimination ability similar to that of the CTI in PE evaluations. Despite the different cut-off values (STI =1.58 *vs.* CTI =2.72), the sensitivity and specificity were both high (0.93 and 0.95 *vs.* 0.93 and 0.97). Due to concerns regarding ionizing radiation in CT, regular examinations of outpatient PE patients has been lacking. The technical advantage of ST is that this approach can fully depict the characterized configuration of PE without radiation. From a historical perspective, diagnostic results based on the STI have been consistent with the conventional assessment criteria in terms of the CTI, allowing for evaluation data continuity and a combined application. From a future perspective, the STI could be an effective alternative indicator to the CTI, allowing for the probability of a novel radiation-free evaluation model based on ST, especially for the early diagnosis of PE. Compared with previous studies, our sample size was significant larger, and the metric index was derived from CT images, rather than ST images. We focused on not only the application of a specific ST scan device but how this ST method changes the PE evaluation field.

We also demonstrated that the STI had a strong Pearson correlation with the CTI. Although the sample size increased from 42 to 371, the correlation coefficients positively increased from 0.85 to 0.91. The correlation coefficient does not decline with an increase in the number of patients. The strong correlation showed satisfactory diagnostic consistency between the surface and internal parameters in PE evaluations. Based on the fitted formula and such a relatively large sample, STI =1.67 can be

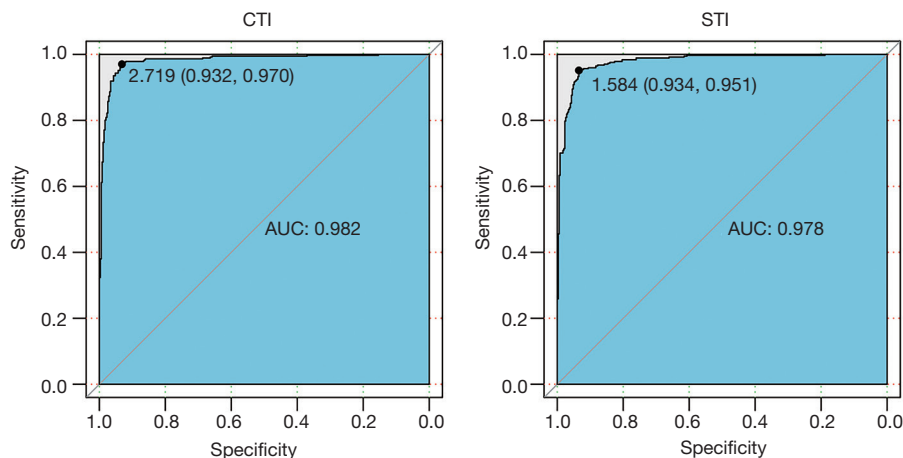


Figure 4 Optimum discriminatory values of the computed tomography index (CTI) and surface topography index (STI). Receiver-operating characteristic curves showed that STI =1.58 (sensitivity: 0.93, specificity: 0.95) could be considered equivalent to CTI =2.72 (sensitivity: 0.93, specificity: 0.97).

considered equivalent to the golden standard of CTI=3.25 as a novel threshold for medical intervention. ST can be used repeatedly and has its own unique advantage in long-term follow up. The STI is an encouraging metric that could facilitate the generalization of this radiation-free technique and reduce the radiation hazards associated with CT scans.

Compared with other similar studies (5-7), the correlation coefficients were similar and the conclusions were consistent, which was expected, because calculations of the STI and CTI are similar. The CTI has been the standard metric for PE evaluations since 1987 (3). A novel metric could inevitably follow this classic index. The main differences in the formula parameters between the STI and CTI are the thicknesses of the ribs, sternum, and thoracic vertebrae. All bony structures in the chest wall have small individual differences among children and grow slowly with age. However, previous studies do not provide enough evidence regarding the diagnostic accuracy of the STI and are limited by the number of patients, such as 5 cases and 12 cases in 2 separate studies (4,5). Our results, which are based on a larger sample size, support the conclusions more reliably.

A unified metric is ideal to facilitate comparisons of data from multiple centers and different periods. The CTI is also known as the Haller index (HI) (3). With a clear definition, the parameters involved in the HI could also be obtained from radiographs, such as radiograph Haller index (rHI) (7). Similarly, the parameters captured by the optical systems could also be obtained from other chest wall images, such as CT and magnetic resonance imaging (MRI). In this case, a novel measuring method will not produce a new index. On the contrary, the 3 indexes in previous studies, the optical Haller index (5), the Index 3d scan (I3ds) (6), and the Optical Index (OI) (7), involved the same parameters and calculations. The reason for this confusion was that the indexes were named after the method used to measure the parameters, rather than the described object of the parameters. The physical signs of PE deformities are visible on the surface. The characteristic configuration of PE is extremely similar to topography from basin to Grand Canyon. The data from optical imaging systems were high-resolution topographic information. Therefore, we coined the term "surface topography index" to indicate that featured surface data from optical systems actually represent topographic information of PE deformities.

There are 3 main challenges in PE deformity evaluations. First, PE deformities involve 3 dimensions (1). For an

accurate severity assessment, comprehensive 3D data are essential. Second, the geometric profile of PE deformities changes over time. PE deformity progression requires long-term monitoring and regular assessments over the disease duration. Third, the contour, scope, and depth of PE deformities vary across individuals. The characterized surface depression of PE deformities varies from cup shaped to Grand Canyon shaped. Given the challenges above, PE deformity evaluations have remained unresolved (9).

The appearance of PE was first depicted in the portrayal of Leonardo da Vinci in 1510 (10). However, painting and photographic images are not sufficient to portray 3D components of PE deformities. In early 1981, moiré phototopography-applied optics was used to accurately measure PE contours (11). Over time, this preliminary study remained unpopular for various reasons. The main reason is generally because the diagnosis and treatment of PE is still in its primary stage. In the 1980s, traumatic Ravitch surgery is the mainstream of the era. Scholars have noticed that the appearances of PE are different. Though complex appearance means greater trauma and more costal cartilage is removed during surgery, complex deformities can be treated by traumatic surgery. Contours are not the focus. Now, minimally invasive repair of pectus excavatum has been the optimal surgery plan. Minimally invasive repairs do not remove costal cartilage and has higher requirements on patient subtypes and operation timing than Ravitch surgery. Therefore, the dynamic monitoring of PE contours, such as symmetry changes, subtype classification and early intervention have become especially important.

Currently, CT scan is the main technique to assess PE severity via the CTI, especially in the preoperative evaluation (12,13). However, radiation exposure remains the main reason to seek optimization and alternatives to CT scans. In the optimization scheme, Khanna *et al.* found that the CTI derived from radiography correlated strongly with CTI and suggested that chest radiography is sufficient for PE evaluations (13). Messerli-Odermatt *et al.* demonstrated that low-dose CT is excellent for assessing the CTI (14). MRI and optical imaging systems are under consideration as alternatives for CT (5-7,15-18). Optical imaging systems are good for capturing high-resolution 3D information at a high-speed (7,17,18). On the premise of a scientific index system, ST scans will be an optimal objective measurement for PE deformity.

The present study has limitations that warrant attention. First, most healthy children do not undergo CT examinations; therefore, the control group included non-PE patients,

but not healthy children. Second, we did not specifically stratify the PE patients by age and deformity severity. In this preliminary study, the sample size had priority over exact match. Finally, as this study was a retrospective study at a single center, racial differences in PE must be considered when the results are validated or applied.

Early diagnosis, early treatment, and frequent monitoring are important in modern medicine. For PE, early screening and frequent evaluations could have a significant effect on the progression and prognosis of PE deformities. 3D ST scanning offers a high-speed, objective, and radiation-free measurement method. Surface information of the chest wall, including both parameter measurements and detailed depictions, could be acquired by ST scans based on optical systems. Surface information can provide insight into the internal structure of PE deformities. Moreover, the STI does not change due to the use of different scales in PE patients. Universal and standardized guidelines for PE evaluation or management are lacking. The STI could facilitate the generalization of this radiation-free evaluation technique and reduce the radiation hazards associated with CT scans, especially for the early diagnosis and long-term follow up of PE.

Conclusions

The STI has comparative discrimination ability in PE diagnosis and severity assessment when used with the standard CTI. The STI as a novel index is not only an ideal evaluation metric of PE deformity but also a objective trait in PE patients just as weight and height for everyone.

Acknowledgments

Funding: This work was supported by Natural Science Foundation of Guangdong Province (2020A1515010005), Fund from Guangzhou Women and Children's Medical Center (CWCMC2020-6-012), and National Key R&D Program of China (2018YFC1311900).

Footnote

Reporting Checklist: The authors have completed the STARD reporting checklist. Available at <https://dx.doi.org/10.21037/tp-21-282>

Data Sharing Statement: Available at <https://dx.doi.org/10.21037/tp-21-282>

Conflicts of Interest: All authors have completed the ICMJE uniform disclosure form (available at <https://dx.doi.org/10.21037/tp-21-282>). The authors have no conflicts of interest to declare.

Ethical Statement: The authors are accountable for all aspects of the work in ensuring that questions related to the accuracy or integrity of any part of the work are appropriately investigated and resolved. All procedures performed in this study involving human participants were in accordance with the Declaration of Helsinki (as revised in 2013). This retrospective study was approved by the institutional review board of Guangzhou Women and Children's Medical Center on November 18, 2016 (No. 2016111876). Written informed consent was obtained from the patients or their parent.

Open Access Statement: This is an Open Access article distributed in accordance with the Creative Commons Attribution-NonCommercial-NoDerivs 4.0 International License (CC BY-NC-ND 4.0), which permits the non-commercial replication and distribution of the article with the strict proviso that no changes or edits are made and the original work is properly cited (including links to both the formal publication through the relevant DOI and the license). See: <https://creativecommons.org/licenses/by-nc-nd/4.0/>.

References

1. Kelly RE Jr. Pectus excavatum: historical background, clinical picture, preoperative evaluation and criteria for operation. *Semin Pediatr Surg* 2008;17:181-93.
2. Shi R, Xie L, Chen G, et al. Surgical management of pectus excavatum in China: results of a survey amongst members of the Chinese Association of Thoracic Surgeons. *Ann Transl Med* 2019;7:202.
3. Haller JA Jr, Kramer SS, Lietman SA. Use of CT scans in selection of patients for pectus excavatum surgery: a preliminary report. *J Pediatr Surg* 1987;22:904-6.
4. Brenner DJ, Hall EJ. Computed tomography-an increasing source of radiation exposure. *N Engl J Med* 2007;357:2277-84.
5. Poncet P, Kravarusic D, Richart T et al. Clinical impact of optical imaging with 3-D reconstruction of torso topography in common anterior chest wall anomalies. *J Pediatr Surg* 2007;42:898-903.
6. Glinkowski W, Sitnik R, Witkowski M, et al. Method of pectus excavatum measurement based on structured light

- technique. *J Biomed Opt* 2009;14:044041.
7. Taylor JS, Madhavan S, Szafer D, et al. Three-dimensional optical imaging for pectus excavatum assessment. *Ann Thorac Surg* 2019;108:1065-71.
 8. Wang H, Wang FH, Si WY, et al. The application of 3-D scanning in the diagnosis and evaluation of pectus excavatum. *Chin J Thorac Cardiovasc Surg* 2018;34:284-7.
 9. Nuss D, Kelly Jr. RE, Croitoru DP, et al. A 10-year review of a minimally invasive technique for the correction of pectus excavatum. *J Pediatr Surg* 1998;33:545-52.
 10. Ashrafiyan H. Leonardo da Vinci and the first portrayal of pectus excavatum. *Thorax* 2013;68:1081.
 11. Shochat SJ, Csongradi JJ, Hartman GE, et al. Moiré phototopography in the evaluation of anterior chest wall deformities. *J Pediatr Surg* 1981;16:353-7.
 12. Nakagawa Y, Uemura S, Nakaoka T, et al. Tanaka. Evaluation of the Nuss procedure using pre- and postoperative computed tomographic index. *J Pediatr Surg* 2008;43:518-21.
 13. Khanna G, Jaju A, Don S, et al. Comparison of Haller index values calculated with chest radiographs versus CT for pectus excavatum evaluation. *Pediatr Radiol* 2010;40:1763-7.
 14. Messerli-Odermatt O, Serrallach B, Gubser M, et al. Chest X-ray Dose Equivalent Low-dose CT With Tin Filtration: Potential Role for the Assessment of Pectus Excavatum. *Acad Radiol* 2020;27:644-50.
 15. Humphries CM, Anderson JL, Flores JH, et al. Cardiac magnetic resonance imaging for perioperative evaluation of sternal eversion for pectus excavatum. *Eur J Cardiothorac Surg* 2013;43:1110-3.
 16. Hebal F, Port E, Hunter CJ, et al. A novel technique to measure severity of pediatric pectus excavatum using white light scanning. *J Pediatr Surg* 2019;54:656-62.
 17. Wells JC, Stocks J, Bonner R et al. Acceptability, Precision and Accuracy of 3D Photonic Scanning for Measurement of Body Shape in a Multi-Ethnic Sample of Children Aged 5-11 Years: The SLIC Study. *PLoS One* 2015;10:e0124193.
 18. Wells JC, Ruto A, Treleaven P. Whole-body three-dimensional photonic scanning: a new technique for obesity research and clinical practice. *Int J Obes (Lond)* 2008;32:232-8.

(English Language Editor: R. Scott)

Cite this article as: Wang H, Liu W, Zhang DY, Si WY, Yang QL, Lu LW, Wang FH, Li L, Wang Q, Xia HM. Surface topography index: a novel deformity severity assessment index for pectus excavatum. *Transl Pediatr* 2021;10(8):2044-2051. doi: 10.21037/tp-21-282